PCCP

A ligand substitution reaction of oxo-centred triruthenium complexes assembled as monolayers on gold electrodes

Akira Sato, Masaaki Abe,* Tomohiko Inomata, Toshihiro Kondo, Shen Ye, Kohei Uosaki* and Yoichi Sasaki*

Division of Chemistry, Graduate School of Science, Hokkaido University, Kita-ku, Sapporo 060-0810, Japan

Received 16th February 2001, Accepted 20th June 2001
First published as an Advance Article on the web 24th July 2001

A terminal ligand-substitution reaction at triruthenium redox centres within monolayer films is investigated. For this purpose, a new redox-active trinuclear ruthenium complex containing one carbonyl ligand at a terminal site, $[Ru_3(O)(CH_3COO)_6(CO)(mpy)(C10PY)]$ (mpy = 4-methylpyridine, C10PY = $\{(NC_5H_4)CH_2NHC(O)(CH_2)_{10}S-\}_2$) **1**, has been chemically adsorbed onto a gold electrode surface with a disulfide-alkyl spacer C10PY. Densely packed monolayers of complex **1** on Au electrodes (surface coverage, $\Gamma(Ru_3) = 1.8 \times 10^{-10}$ mol cm^{-2}) display the $\{Ru^{II}–CO\}Ru^{III}Ru^{III}/\{Ru^{III}–CO\}Ru^{III}Ru^{III}$ couple at $E_{1/2} = +0.61$ V *vs.* Ag–AgCl in a 0.1 mol dm^{-3} $HClO_4$ aqueous solution. Upon electrochemical oxidation of the adsorbed complex at +0.80 V, where the triruthenium carbonyl complex is in the oxidized form $\{Ru^{III}–CO\}Ru^{III}Ru^{III}$, the coordinated CO is replaced by an aqua ligand present in the bulk phase, which is followed by cyclic voltammetry at appropriate electrolysis time intervals. During 8000 s of electrolysis, *ca.* 67% of the initially assembled carbonyl complexes are converted to the triruthenium aqua complexes, while *ca.* 25% desorbed from the electrode surface.

Introduction

There is presently much interest in the development of thin films displaying specific functions in view of both fundamental interest and applications. In particular, preparation of self-assembled monolayers or spontaneously adsorbed monolayers is a highly useful approach to yield structurally ordered molecular arrays on atomically smooth metal surfaces.[1–5] Inorganic coordination compounds can be used to generate a wide range of monolayers with metal-based physical and chemical properties,[6–17] including heterogeneous electron-transfer, photophysical processes, sensing and catalysis. One of the intriguing and fundamental aspects of coordination compounds is solution ligand-substitution reaction or exchange dynamics. However, for surface-confined metal complexes, this issue has been scarcely addressed in the literature.[18–20]

In this work, we examined interfacial ligand substitution reactions occurring in monolayers of a new triruthenium complex $[Ru_3(O)(CH_3COO)_6(mpy)(CO)(C10PY)]$ **1**, where mpy = 4-methylpyridine and C10PY = $\{(NC_5H_4)$-$CH_2NHC(O)(CH_2)_{10}S-\}_2$. The structural formula of the complex is illustrated in Fig. 1.

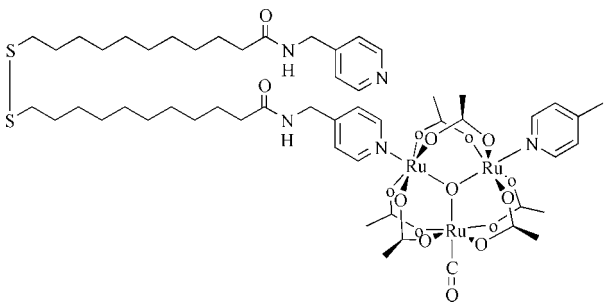

Fig. 1 Structural formula of complex **1**.

The choice of the metal complex is based on our recent interest in the development of functionallized monolayers utilizing redox-active dinuclear[21–23] and trinuclear[24–26] metal complexes. Across the series, oxo-centred triruthenium complexes of the type $[Ru_3(O)(RCOO)_6L_3]^{0/+}$ (RCOO = a carboxylate anion, L = a monodentate terminal ligand)[27] may be regarded as highly attractive motifs for the preparation of functionallized mono- and multilayer architectures due to their known chemical properties including reversible multistep/multielectron redox processes,[28–30] ligand-mediated electron-transfers,[31–33] the formation of supramolecular structures,[34–38] ligand-substitution reactions in solution[39–41] and homogeneous catalysis.[42,43]

It has been established for $[Ru_3(O)(CH_3COO)_6(CO)(py)_2]$ (py = pyridine), the analog of **1**, that the CO ligand on the Ru^{II} centre can be replaced by a co-existing ligand (such as a solvent molecule) upon chemical oxidation of Ru^{II}[28] or UV-irradiation[34] in solution. We find in this work that electrochemical oxidation also triggers the CO-substitution reaction of the triruthenium complexes assembled on gold electrodes. Knowledge about ligand-substitution reactions of metal complexes in monolayers will also provide significant insights into the construction of multilayers based on metal–ligand coordination bonds.[44–46] We describe here the electrochemical behaviour and the CO/aqua ligand substitution reaction of the triruthenium carbonyl complex **1** assembled on Au electrode surfaces. The preparation, characterization and electrochemical properties of **1** are also detailed.

Experimental

Materials

Reagents and solvents used were of commercially available reagent-grade quality unless otherwise stated. $RuCl_3 \cdot 3H_2O$

 DOI: 10.1039/b101561n

was purchased from Shiga Kikinzoku Co. Acetonitrile used for electrochemical measurements was distilled from CaH_2 under argon. Tetrahydrofuran (THF) was distilled from sodium/benzophenone under argon. Silica gel (Wako gel C-300HG, Wako Chemicals) was used for column chromatography. Ultrapure water was obtained by using a Milli-Q water purification system (Yamato, WQ-500).

The ligand (C10PY) was prepared according to the method reported previously.[26] A triruthenium complex $[Ru_3(O)(CH_3CO_2)_6(THF)_2(CO)]\cdot 2THF$ (THF = tetrahydrofuran) was prepared as described in ref. 24.

Physical methods

Infrared spectra were recorded on a Hitachi 270-50 infrared spectrophotometer using KBr disks. UV–VIS spectra were obtained with a Hitachi U-3410 spectrophotometer. ^1H NMR spectra were recorded on a JEOL JNM-EX 270 NMR spectrometer at 270.15 MHz. All chemical shifts are reported as δ values downfield from an internal standard of tetramethylsilane (TMS) for use with $CDCl_3$ and CD_3CN or 3-(trimethylsilyl)-propane sulfonic acid, sodium salt (DSS) for use with D_2O. Fast-atom bombardment (FAB) mass spectra were recorded on a JEOL JMS-HX110 mass spectrometer in the positive-ion mode and nitrobenzyl alcohol (NBA) was used as a matrix. FAB mass spectrometry and elemental analysis were performed at the Center for Instrumental Analysis, Hokkaido University.

Electrochemistry of triruthenium complexes dissolved in solution

Cyclic voltammetry and differential-pulse voltammetry were performed using a Hokuto Denko Automatic Polarization System HZ-3000. A working electrode, a counter electrode and a reference electrode were glassy carbon, platinum coil and Ag–AgCl (sat. NaCl), respectively. The electrochemical measurements were conducted at 20 °C under an argon atmosphere using acetonitrile solutions containing 0.1 mol dm^{-3} $(n\text{-}Bu_4N)PF_6$ as a supporting electrolyte and a metal complex with 0.5–1.0 mmol dm^{-3} concentration. Under these conditions, the half-wave potential ($E_{1/2}$) of the ferrocene/ferrocenium couple (Fc/Fc^+) was observed at +0.435 V *vs.* Ag–AgCl with the peak-to-peak separation (ΔE_p) of 60 mV at a scan rate of 100 mV s^{-1}.

Electrochemistry of monolayer-coated Au electrodes

The Au(111) electrode used in this study was prepared according to the method previously described.[47,48] The roughness factor of the Au(111) electrode surface was 1.2 (the surface area = 0.0595 cm^2) based on the observed charge in the cyclic voltammogram for the reduction of gold oxide using 0.1 mol dm^{-3} H_2SO_4 solution. The roughness factor of a polycrystalline gold electrode used in this study was estimated to be 1.4. Prior to the surface modification, the Au electrodes were washed with pure water, annealed in a hydrogen flame and quenched with Milli-Q water.

Densely packed monolayers were prepared by immersing the Au electrode into an ethanol solution (5 cm^3) of complex **1**, concentration 0.1 mmol dm^{-3}, for 2 days in the dark at 20 °C. Prior to the electrochemical measurements, the modified Au electrode was rinsed with ethanol and Milli-Q water.

The monolayer-coated gold electrodes were placed in an electrode holder made from Kel-F so that only one face of the substrate formed a meniscus with an electrolyte solution. A platinum wire and an Ag–AgCl (sat. NaCl) were used as counter and reference electrodes, respectively. Cyclic voltammetry for monolayer-coated Au electrodes was conducted using 0.1 mol dm^{-3} $HClO_4$ aqueous solutions at room temperature under an argon atmosphere at scan rates 50–500 mV s^{-1}. Prior to the electrochemical measurements, the $HClO_4$ aqueous solution was deaerated by bubbling argon gas for 30 min with stirring.

Preparations

$[Ru_3(O)(CH_3CO_2)_6(CO)(mpy)(THF)]$. This complex was prepared by an analogous method to that for $[Ru_3(O)(CH_3COO)_6(CO)(py)(H_2O)]$.[34] To a methanol/dichloromethane (1 : 1 v/v) solution (50 cm^3) containing $[Ru_3(O)(CH_3COO)_6(CO)(THF)_2]\cdot 2THF$[24] (232 mg, 0.234 mmol) was added a 0.9 equivalent of mpy (20 mg, 0.215 mmol) with stirring at room temperature. The mixture was stirred for 64 h. After the solvent was removed by a rotary evaporator, the residue was purified by column chromatography using silica gel (ϕ2.0 × 33 cm). Elution with 1–2% methanol/dichloromethane afforded three bands on the column. The first band was eluted by 1% methanol/dichloromethane, while the second and the third bands were eluted by 2% methanol/dichloromethane. After the elution was completed, the solvent was removed from each fraction. On the basis of ^1H NMR spectroscopy, the second fraction contains $[Ru_3(O)(CH_3COO)_6(CO)(mpy)(S)]$ where S represents CH_3OH and/or H_2O, while the first and the third fractions contain known complexes, $[Ru_3(O)(CH_3COO)_6(CO)(mpy)_2]$[24] and $[Ru_3(O)(CH_3COO)_6(CO)S_2]$,[49] respectively. Recrystallization of the solid from the second band from THF/n-pentane afforded a deep blue crystalline solid, which was collected by filtration, washed with n-pentane and dried under vacuum. Yield, 72.6 mg (35.8%). Analysis: Calcd. for $C_{23}H_{33}NO_{15}Ru_3$: C, 31.87; H, 3.84; N, 1.62%. Found: C, 32.15; H, 3.89; N, 1.54%. Selected IR data (cm^{-1}, KBr pellet): 1942 vs (ν(CO, terminal)), 1614 vs ($\nu_{asym}(COO^-)$), 1576 s ($\nu_{asym}(COO^-)$), 1426 vs ($\nu_{asym}(COO^-)$). ^1H NMR (D_2O, 20 °C, *vs.* DSS): δ 9.43 (2 H, d, mpy 2,6-H), 8.10 (2 H, d, mpy 3,5-H), 3.74 (5.8 H, m, THF), 2.82 (3 H, s, mpy CH_3), 1.97 (6 H, s, acetate CH_3), 1.95 (6 H, s, acetate CH_3), 1.88 (5.8 H, m, THF), 1.73 (6 H, s, acetate CH_3). UV–VIS (acetonitrile): λ_{max}/nm (ε/mol dm^{-3} cm^{-1}) 582 (4200).

$[Ru_3(O)(CH_3CO_2)_6(CO)(mpy)(C10PY)]$ 1. A mixture of complex $[Ru_3(O)(CH_3CO_2)_6(CO)(mpy)(THF)]$ (175 mg, 0.21 mmol) and C10PY[26] (402 mg, 0.65 mmol) was dissolved in argon-purged methanol/dichloromethane (60 cm^3, 1 : 2 v/v). The solution was stirred for 40 h at room temperature under argon. The resultant crude solid was purified by column chromatography using silica gel (ϕ 2.7 cm × 21 cm) with 2% methanol/dichloromethane as an eluant and, during the column chromatography, the methanol content was gradually increased up to 6%. A total of seven bands (all deep blue in colour) appeared on the column. The solvent was removed under a reduced pressure to remain deep blue solid for each of the samples. ^1H NMR spectra revealed that the solid sample from the 6th band contain the desired complex **1**. The solid was recrystallized from THF/n-pentane, collected by filtration, washed with n-pentane and dried under vacuum. Yield, 16 mg (5.4%). Analysis: Calcd. for $C_{53}H_{79}N_5O_{16}Ru_3S_2\cdot H_2O$: C, 44.59; H, 5.72; N, 4.91; S, 4.49%. Found: C, 44.30; H, 5.42; N, 4.75; S, 4.24%. Selected IR data (cm^{-1}, KBr pellet): 2956 w ($\nu_{asym}(CH_2)$), 2928 vw ($\nu_{sym}(CH_2)$), 1944 vs (ν(CO, terminal), 1652 m (ν(CO, C10PY)), 1610 vs ($\nu_{asym}(COO^-)$), 1574 m ($\nu_{asym}(COO^-)$), 1424 vs (ν_{sym} (COO^-)). FAB-MS (NBA as a matrix): m/z = 1382 $[M–CO]^+$, 1289 $[M–CO–mpy]^+$. ^1H NMR ($CDCl_3$, 20 °C, *vs.* TMS): δ 9.02 (2 H, d, mpy β-H), 8.99 (2 H, d, coord py α-H), 8.54 (2 H, d, py α-H), 7.92 (2 H, d, coord py β-H), 7.86 (2 H, d, mpy α-H), 7.18 (2 H, d, free py β-H), 6.32 (1 H, br, t, free py–CH_2–N*H*–CO–), 5.96 (1 H, br, t, coord py–CH_2–N*H*–CO–), 4.94 (2 H, d, coord py–C*H*$_2$–N*H*–),

4.46 (2 H, d, free py–CH_2–NH–), 2.67 (4 H, t, –CH_2–SS–CH_2–), 2.87 (3 H, s, mpy CH_3), 2.37 (2 H, t, –CH_2–CO–), 2.26 (2 H, t, –CH_2–CO–), 2.09 (6 H, s, acetate CH_3), 2.08 (6 H, s, acetate CH_3), 1.81 (6 H, s, acetate CH_3), 1.55–1.75 (16 H, br, m, –CH_2–), 1.25–1.45 (16 H, br, m, –CH_2–). UV–VIS (acetonitrile): λ_{max}/nm (ε/mol dm^{-3} cm^{-1}): 584 (8900), 333 (12 000), 276 (sh, 21 000), 226 (sh, 43 000).

Results and discussion

Preparation, characterization and electrochemical properties of complex 1

In this study, a molecular adsorbate containing a disulfide group, **1** (Fig. 1), was isolated and then monolayers were formed on either an Au(111) electrode or a polycrystalline Au electrode surface.

Complex **1** was prepared from a solvated complex $[Ru_3(O)(CH_3COO)_6(CO)(mpy)(THF)]$ and a disulfide alkyl ligand C10PY through the terminal ligand substitution reaction (THF → C10PY). The complex is isolated in the mixed valent form (II,III,III), in which the divalent state is localized on the ruthenium centre bound to CO, *e.g.*, {Ru^{II}–CO}Ru^{III}Ru^{III}.[30,50] One of the two pyridyl groups in C10PY is bonded to a ruthenium(III) centre while the other is free from coordination. Column chromatographic procedures (silica gel) were required to isolate **1** in a pure form. A ^{1}H NMR spectrum (270.05 MHz, $CDCl_3$) exhibited three singlets with equal intensities due to acetate methyl signals {δ 1.81 (6H), 2.08 (6H) and 2.09 (6H) *vs.* TMS) as expected. An infrared spectrum of **1** (KBr pellet) contained a strong absorption peak due to ν(CO) of a terminal carbonyl ligand (1944 cm^{-1}) together with the asymmetric (1610 and 1574 cm^{-1}) and symmetric (1424 cm^{-1}) stretches of bridging acetate moieties. An additional ν(CO) band ascribed to carbonyl moieties in C10PY was observed at 1625 cm^{-1}. Fast-atom bombardment (FAB) mass spectrometry afforded a parent envelop at m/z = 1382 ([M–CO]$^+$) with fragment peaks corresponding to species with a successive loss of terminal and bridging ligands. An electronic absorption spectrum of **1** in acetonitrile displayed two intense absorption bands in the visible region (λ_{max} = 584 and 333 nm) together with more intense shoulders in the UV region; overall spectral features matched well those of known carbonyl-containing triruthenium(II,III,III) analogues, $[Ru_3(O)(CH_3COO)_6(CO)L_2]$ (L = H_2O, CH_3OH and pyridine derivatives).[28,30,49]

In general, triruthenium complexes of this type show multistep redox processes in solution. Redox properties of **1** as well as $[Ru_3(O)(CH_3COO)_6(mpy)(CO)(H_2O)]$ were examined by cyclic voltammetry using 0.1 mol dm^{-3} (n-Bu_4N)PF_6–acetonitrile ([complex] = 1.0 mmol dm^{-3}) with a glassy carbon working electrode. Electrochemical data and wave assignments are summarized in Table 1.

In the potential range between +2.0 and −2.0 V *vs.* Ag–AgCl, four consecutive one-electron waves associated with reduction/oxidation processes were observed. The assignment of the redox waves is based on comparison of redox data for a closely related complex with one terminal CO, *e.g.*, $[Ru_3(O)(CH_3COO)_6(py)_2(CO)]$ (py = pyridine), established previously.[50] The mixed-valent complex {Ru^{II}–CO}Ru^{III}Ru^{III} can be reversibly oxidized to {Ru^{III}–CO}Ru^{III}Ru^{III} and {Ru^{III}–CO}Ru$^{III.5}$Ru$^{III.5}$, and is reduced reversibly to {Ru^{II}–CO}Ru$^{II.5}$Ru$^{II.5}$ and irreversibly to {Ru^{II}–CO}Ru^{II}Ru^{II}.

Electrochemistry of monolayers derived from 1

Monolayers of **1** have been prepared by immersing gold electrodes in a solution containing the complex under the conditions described in the Experimental section. The disulfide alkyl ligand C10PY links the $\{Ru_3(O)(CH_3COO)_6(mpy)(CO)\}$ moiety and the electrode surface. Cyclic voltammograms for the monolayer deposited on a polycrystalline gold electrode are shown in Fig. 2. Electrochemical data are summarized in Table 2.

The {Ru^{II}–CO}Ru^{III}Ru^{III}/{Ru^{III}–CO}Ru^{III}Ru^{III} couple is observed at $E_{1/2}$ = +0.61 V *vs.* Ag–AgCl with ΔE_p = 70 mV in 0.1 mol dm^{-3} $HClO_4$ aq. solution. The redox potential is similar to the corresponding redox potential of **1** dissolved in acetonitrile (Table 1). In this study, electrochemical measurements were attained under highly acidic conditions (pH 1.0) to detect the highly positive redox wave.

Evidence of surface-confined redox centres is obtained from the observation of a linear correlation of anodic and cathodic peak currents against scan rates,[51] as shown in the inset of Fig. 2. The shape of the wave is independent of the scan rate studied (50–500 mV s^{-1}).

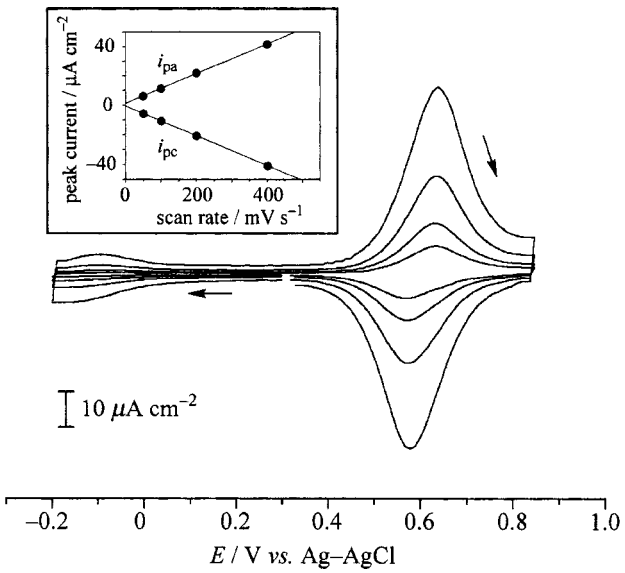

Fig. 2 Cyclic voltammograms for monolayers of **1** assembled on the polycrystalline Au electrode in 0.1 mol dm^{-3} $HClO_4$ aqueous solution at 20 °C in the electrode potential region between −0.25 and +0.85 V *vs.* Ag–AgCl. A platinum wire is used for the counter electrode. Scan rate = 50, 100, 200 and 400 mV s^{-1}. Inset: A linear correlation of current intensities of the anodic and cathodic waves (i_{pa} and i_{pc}, respectively) with the scan rate.

Table 1 Electrochemical data of $[Ru_3(O)(CH_3COO)_6(mpy)(CO)(H_2O)]^{n+}$ and $[Ru_3(O)(CH_3COO)_6(mpy)(CO)(C10PY)]^{n+}$ (**1** when n = 0) in 0.10 mol dm^{-3} (n-Bu_4N)PF_6–acetonitrile (20 °C)[a]

	$E_{1/2}$[b]/V *vs.* Ag–AgCl (ΔE_p[c]/mV)			
Total charge (n)[d]	(−2/−1)	(−1/0)	(0/+1)	(+1/+2)
$[Ru_3(O)(CH_3COO)_6(mpy)(CO)(H_2O)]^{n+}$	−1.72 (120)	−0.75 (70)	+0.69 (80)	+1.37 (80)
$[Ru_3(O)(CH_3COO)_6(mpy)(CO)(C10PY)]^{n+}$ (**1** when n = 0)	−1.82[e]	−0.86 (60)	+0.66 (60)	+1.29 (100)

[a] Scan rate = 200 mV s^{-1}. [b] Half-wave potential, $E_{1/2} = (E_{pa} + E_{pc})/2$, where E_{pa} and E_{pc} are anodic and cathodic peak potentials, respectively. [c] Peak-to-peak separation, $\Delta E_p = E_{pa} - E_{pc}$. [d] Ru oxidation states: {Ru^{II}–CO}Ru^{II}Ru^{II} for n = −2; {Ru^{II}–CO}Ru$^{II.5}$Ru$^{II.5}$ for n = −1; {Ru^{II}–CO}Ru^{III}Ru^{III} for n = 0; {Ru^{III}–CO}Ru^{III}Ru^{III} for n = +1; {Ru^{III}–CO}Ru$^{III.5}$Ru$^{III.5}$ for n = +2. [e] Cathodic peak potential for irreversible process.

Table 2 Electrochemical data for monolayers of triruthenium carbonyl complex **1** and electrochemically-generated monolayers of triruthenium aqua complexes on polycrystalline Au electrodes (20 °C)[a]

	Monolayers of **1**	Monolayers of triruthenium aqua complex
$E_{1/2}$[b]/V *vs.* Ag–AgCl	+0.61	−0.09
ΔE_p[c]/mV	60	70
ΔE_{fwhm}[d]/mV	150[e]	200[f]
$\Gamma(Ru_3)$[g]/mol cm^{-2}	1.8×10^{-10}[e]	1.2×10^{-10}[f]

[a] In 0.10 mol dm^{-3} $HClO_4$ aqueous solution, scan rate = 100 mV s^{-1}. [b] Half-wave potential, *vs.* Ag–AgCl. [c] Peak-to-peak potential. [d] Full-width at half-maximum value. [e] Obtained from the cathodic wave. [f] Obtained from the anodic wave. [g] Surface coverage of the triruthenium redox centres.

The surface coverage of **1** on a gold surface, $\Gamma(Ru_3)$, was determined to be 1.8×10^{-10} mol cm^{-2}, by integrating the charge under the redox wave at +0.61 V. This is consistent with the theoretical value expected for close-packed monolayers, 1.7×10^{-10} mol cm^{-2}, assuming a molecular area of *ca.* 114 Å^2 based on X-ray crystallographic data of a structurally similar complex, $[Ru_2Mg(O)(CH_3COO)_6(cpy)_2(H_2O)]$ (cpy = 4-cyanopyridine).[52] Further, the surface coverage observed here is similar to that of $[Ru_3(O)(CH_3COO)_6(mpy)_2(C10PY)]^+$ monolayers on the Au(111) electrode (1.6×10^{-10} mol cm^{-2}).[26]

The full-width at half-maximum (ΔE_{fwhm}) of the redox wave at +0.61 V (Fig. 2) is estimated to be 150 mV, substantially larger than the predicted value for surface-confined non-interacting redox centres, 90.6 mV.[51] The broad redox wave observed for the present monolayer can be interpreted as a result of repulsive lateral interactions between adjacent redox centres and/or multiple redox potentials due to the different microenvironments of the redox centres within the monolayers. The same magnitude of ΔE_{fwhm} is also observed for the $[Ru_3(O)(CH_3COO)_6(mpy)_2(C10PY)]^+$ monolayer.[26] A constant, non-zero peak-to-peak separation between the anodic and cathodic potentials (ΔE_p), *e.g.*, 70 mV, is observed at scan rates 50–500 mV s^{-1}. The electrochemical response of monolayers of **1** developed on the Au(111) electrode was virtually identical to that of the monolayer formed on the polycrystalline Au electrode described above ($E_{1/2} = 0.61$ V, $\Delta E_p = 70$ mV, $\Delta E_{fwhm} = 160$ mV, $\Gamma(Ru_3) = 1.5 \times 10^{-10}$ mol cm^{-2}). The scan rate dependence of the redox wave beyond 500 mV s^{-1} was not examined in this study.

Electrochemical oxidation process of monolayers derived from 1

Electrochemical one-electron oxidation of surface-confined triruthenium carbonyl centres within monolayers leads to the liberation of the carbonyl ligand and produces triruthenium aqua complexes that are retained on the electrode surface. This substitution reaction of a triruthenium redox centre can be easily monitored by cyclic voltammetry, because redox waves due to two surface species, *e.g.*, complexes *with* carbonyl and *without* carbonyl, appear at considerably different potentials and are easily distinguished as described below. The interfacial ligand substitution reaction is illustrated in Scheme 1.

Cyclic voltammetry was used to monitor the ligand liberation process of **1** assembled on Au electrodes. Fig. 3 shows the sequential variations in the cyclic voltammograms for monolayers of **1** prepared on the polycrystalline Au electrode, obtained at different electrolysis times in 0.1 mol dm^{-3} $HClO_4$ solution.

In this experiment, the electrode potential is maintained at +0.80 V during electrolysis, where the surface-immobilized complexes are in the $\{Ru^{III}–CO\}Ru^{III}Ru^{III}$ oxidation state. The voltammogram recorded prior to the electrolysis (*e.g.*, electrolysis time = 0 s) is labeled as (a) in Fig. 3, which is consistent with the voltammogram in Fig. 2 at a scan rate of 200 mV s^{-1}. Upon electrolysis, the charge under the +0.61 V wave due to surface-confined **1** begins to decrease, while a new wave increases around +0.1 V. This situation can be seen in voltammograms (b) to (e). As mentioned above, the electrolysis at +0.8 V corresponds to the one-electron-oxidation of the Ru^{II} bound by CO, thus leading to a weakening of the Ru–CO bonding, the liberation of CO and concomitant introduction of a co-existing ligand H_2O. Finally, as shown in voltammogram (f), the triruthenium aqua complex becomes dominant as a surface species. The introduction of the aqua ligand to the triruthenium redox centre is supported by the similarity of the redox potential of the new wave to that of CO-free triruthenium complexes $[Ru_3(O)(CH_3COO)_6(\text{pyridine derivatives})_2(H_2O)]^+$ dissolved in solution. For example, $[Ru_3(O)(CH_3COO)_6(mpy)_2(H_2O)]^+$ exhibits the $Ru^{III}Ru^{III}Ru^{III}/Ru^{II}Ru^{III}Ru^{III}$ process at $E_{1/2} = +0.04$ V in 0.1 mol dm^{-3} (n-Bu_4N)PF_6–acetonitrile.[26] We consider that the ligand introduced into the vacant Ru site is the H_2O molecule present in the solution phase and not a pyridyl pendant present in the vicinity of triruthenium groups (see Scheme 1), since the pyridyl group should be protonated under the conditions employed (pH 1). The substitution reaction of **1** assembled as a monolayer is consistent with our previous observation using the FT-IRRAS (Fourier-transform infrared reflection–absorption spectroscopy) technique on a closely related monolayer derived from $[Ru_3(O)(CH_3COO)_6(CO)(MeIm)(C2PY)]$ {MeIm = 1-methylimidazole, C2PY = $\{(NC_5H_4)CH_2NHC(O)(CH_2)_2S–\}_2$},[25] in which a decay in intensity of the ν(CO) absorption band was observed as the electrolysis time increased. A sequential potential sweep in the region between −0.20 and +0.85 V (not shown) was found to result in a decrease in the charge of the redox wave at +0.61 V and concomitant increase of a new wave around −0.1 V. The tiny new wave can be seen around −0.10 V in Fig. 2, most apparently in the CV recorded at 400 mV s^{-1}.

In Fig. 4, voltammetric charges due to the surface-confined triruthenium carbonyl and aqua complexes, represented as Q_{CO} and Q_{aqua}, respectively, are plotted against the electrolysis time. The value of Q_{aqua} was estimated from the anodic charge of the −0.1 V wave, and that of Q_{CO} from the cathodic charge of the +0.61 V wave. The sum of two charges, *e.g.*, $Q_{CO} + Q_{aqua}$, is also included in Fig. 4 to display the variation in the total amount of redox centres attached to the surface during the ligand-substitution reaction.

As seen in Fig. 4, the total charge ($Q_{CO} + Q_{aqua}$) decreased rapidly in the initial stage of the ligand-substitution reaction (*e.g.*, <2000 s), while it remained virtually unchanged to 8000 s of electrolysis. The final total coverage (at 7980 s) corresponds to *ca.* 75% of the initial surface coverage of **1**. The decrease in the total charge corresponds to desorption of redox centres from the gold surface. We tentatively assign the domain of the loss as most likely the disordered phase of the molecules on surface. The electrostatic repulsive force between electrochemically-generated +1 charged redox centres and the gold surface (+0.80 V) would be significant, thus leading to desorption of weakly attached redox centres. It is noted that the additional redox couple ascribed to $Ru^{III}Ru^{III}Ru^{III}/Ru^{III}Ru^{III}Ru^{IV}$ is expected to occur around +1.0 V *vs.* Ag–AgCl for the triruthenium aqua complex as observed for $[Ru_3(O)(CH_3COO)_6(mpy)_2(H_2O)]^+$ in acetonitrile.[26] The onset of the corresponding redox wave is actually seen in the present voltammograms (Fig. 3) in the potential region beyond +0.8 V. After 8000 s of electrolysis, the surface coverage of triruthenium aqua complex was estimated to be 1.2×10^{-10} mol cm^{-2} from the anodic wave, corresponding to 67% of the initial coverage of **1**. At this point, *ca.* 8% (1.5×10^{-11} mol cm^{-2}) of the surface complex still remained as **1**. Invariant total surface coverage during the electrolysis

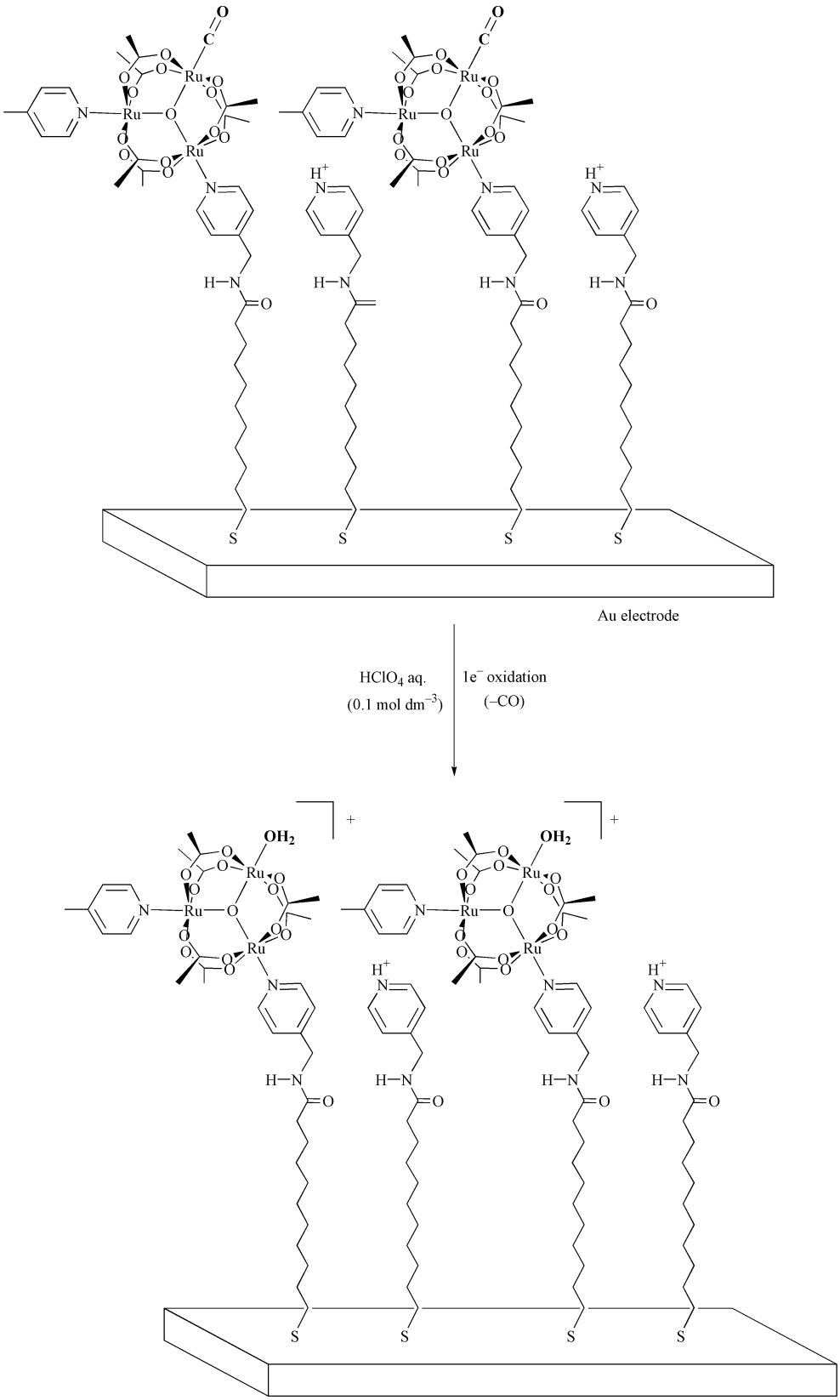

Scheme 1 An ideal representation of monolayers of triruthenium complexes on a gold electrode surface and the CO → H_2O ligand-substitution reaction within the monolayer.

experiment after 2000 s indicates the stable character of the monolayer under highly acidic conditions (pH 1). Identical kinetic behaviour was observed for monolayers prepared on Au(111) electrode.

It is of interest to compare the ligand substitution kinetics of the surface-confined complex to that observed in the solution phase. Kido *et al.* observed that upon irradiation with a Xe lamp (>290 nm) the coordinated CO ligand in $[Ru_3(O)(CH_3COO)_6(py)_2(CO)]$, $[Ru_3(O)(CH_3COO)_6(cpy)_2(CO)]$ and $[Ru_3(O)(CH_3COO)_6(CH_3OH)_2(CO)]$ was replaced by acetonitrile molecule in homogeneous acetonitrile solutions to form $[Ru_3(O)(CH_3COO)_6(py)_2(CH_3CN)]$, $[Ru_3(O)(CH_3COO)_6(cpy)_2(CH_3CN)]$ and $[Ru_3(O)(CH_3COO)_6(CH_3CN)_3]$, respectively.[34,53] The CO → CH_3CN substitution reaction was found to be first-order and rate constants of *ca.* 10^{-4} s^{-1} were

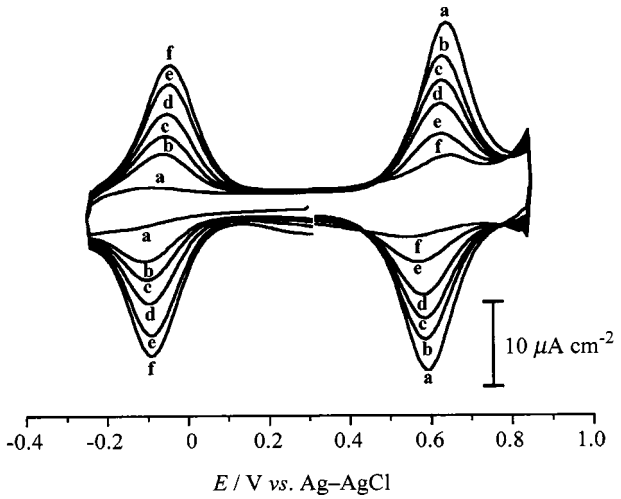

Fig. 3 Sequential variations in cyclic voltammograms for monolayers of **1** assembled on the polycrystalline Au electrode (0.1 mol dm^{-3} $HClO_4$ aq., scan rate = 200 mV s^{-1}) during the course of the electrolysis experiment, showing ligand substitution reaction ($CO \rightarrow H_2O$) at triruthenium redox centres within monolayer films. The Au electrode potential is maintained at +0.8 V *vs.* Ag–AgCl during electrolysis, where the surface-confined triruthenium carbonyl complex is in the oxidized form $\{Ru^{III}–CO\}Ru^{III}Ru^{III}$. Cyclic voltammograms recorded at electrolysis times of 0 (a), 50 (b), 120 (c), 270 (d), 930 (e) and 5980 (f) are presented.

obtained for the series of the complexes. When the first-order kinetic treatment is similarly applied to the present monolayer prepared on the Au(111) electrode, namely, $\ln\{Q_{CO}/(Q_{CO} + Q_{aqua})\}$ *vs.* electrolysis time, the rate constant of $1.4(\pm 0.1) \times 10^{-3}$ s^{-1} ($t_{1/2} = ca.$ 500 s) is obtained. (The kinetic analysis is conducted using data points between 0 and 800 s, during which time *ca.* 73% of the total carbonyl complexes are aquated, and an apparent retardation of the reaction is evident after 800 s.) Unfortunately, there are no kinetic data for oxidation-triggered ligand substitution reaction in the homogeneous phase for direct comparison with the present monolayer case. More detailed comparative kinetic studies on the complexes as a monolayer and in solution are in progress.

Electrochemistry of monolayers containing aqua complexes

Fig. 5 shows cyclic voltammograms for electrochemically-generated (8000 s of electrolysis) triruthenium aqua complex monolayers. The surface-immobilized character of the triruthenium aqua complex is confirmed by the linear correlation between the current intensities of the $Ru^{II}Ru^{III}Ru^{III}/Ru^{III}Ru^{III}Ru^{III}$ couple ($E_{1/2} = -0.09$ V) and scan

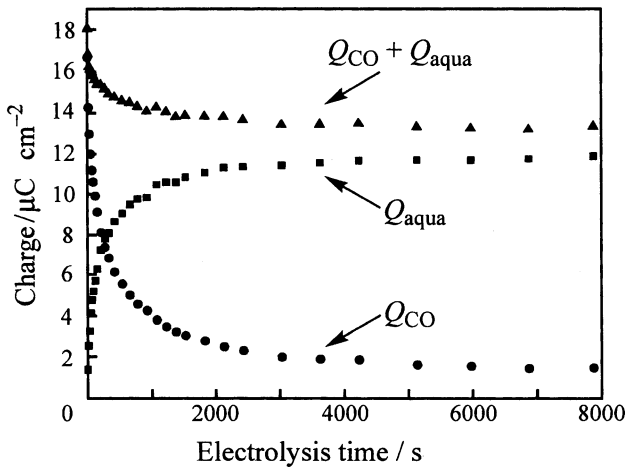

Fig. 4 The variation in the charges of the cyclic voltammetric waves due to the surface-confined triruthenium carbonyl complex **1** (Q_{CO}) and triruthenium aqua complex (Q_{aqua}) as well as the sum of two charges ($Q_{CO} + Q_{aqua}$).

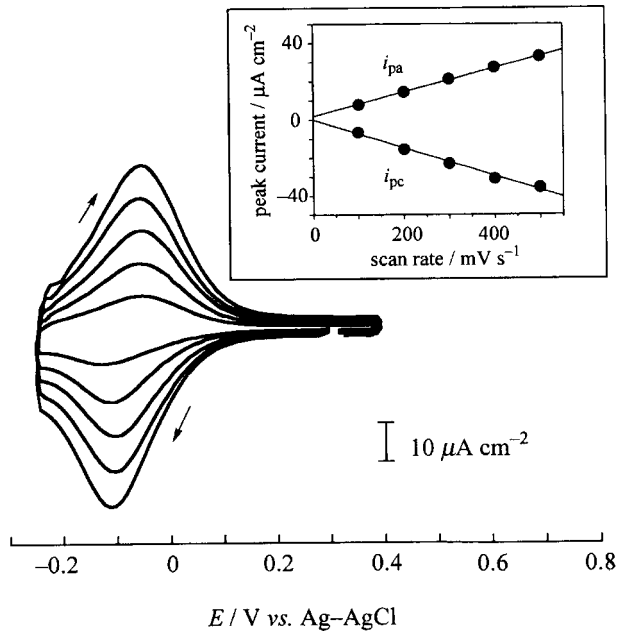

Fig. 5 Cyclic voltammograms for electrochemically-generated monolayers of the aqua complexes on the polycrystalline Au electrode in 0.1 mol dm^{-3} $HClO_4$ aqueous solution at 20 °C in the electrode potential region between −0.25 and +0.40 V *vs.* Ag–AgCl. A platinum wire is used for the counter electrode. Scan rate = 100, 200, 300, 400 and 500 mV s^{-1}. Inset: A linear correlation of current intensities of the anodic and cathodic waves (i_{pa} and i_{pc}, respectively) with the scan rate.

rates (50–500 mV s^{-1}), as shown in the inset of Fig. 5. Electrochemical data for this monolayer are included in Table 2. The much broader ΔE_{fwhm} (200 mV at a scan rate of 100 mV s^{-1}) may infer a more disordered morphology of the electrochemically generated monolayer.

Conclusion

In the present work, we have prepared and examined redox properties of spontaneously adsorbed monolayers of the oxo- and acetato-bridged triruthenium complex possessing one carbonyl terminal ligand $[Ru_3(O)(CH_3COO)_6(mpy)(CO)(C10PY)]$ **1**. The triruthenium carbonyl complex monolayers reveal the $\{Ru^{II}–CO\}Ru^{III}Ru^{III}/\{Ru^{III}–CO\}Ru^{III}Ru^{III}$ couple at +0.61 V for the first potential sweep, while a new wave appears and grows around −0.1 V during the multiple potential cycles or electrolysis at +0.8 V. The new redox wave corresponds to the $Ru^{II}Ru^{III}Ru^{III}/Ru^{III}Ru^{III}Ru^{III}$ couple due to the triruthenium aqua complexes on the electrode surface which are generated through carbonyl substitution reaction upon oxidation. The ligand substitution of metal complexes attached to surfaces is of marked importance and interest in the future design of layer-by-layer multilayer assemblies based on metal–ligand bond formation. Study along this line is currently in progress in our laboratory.

Acknowledgements

This work was supported by Grant-in-Aids for Scientific Research on Priority Area of "Electrochemistry of Ordered Interfaces" (Nos. 09554037 and 09237106), and No. 09740483 from the Ministry of Education, Science, Sports and Culture, Japan. M.A. acknowledges the Sasakawa Scientific Research Grant from The Japan Science Society for the financial support.

References

1 A. Ulman, *Chem. Rev.*, 1996, **96**, 1533.
2 M. J. Esplandiú, H. Hagenström and D. M. Kolb, *Langmuir*, 2001, **17**, 828.

3 C. E. D. Chidsey, *Science*, 1991, **251**, 919.
4 J. J. Hickman, D. Ofer, P. E. Laibinis, G. M. Whitesides and M. S. Wrighton, *Science*, 1991, **252**, 688.
5 R. J. Forster and L. R. Faulkner, *J. Am. Chem. Soc.*, 1994, **116**, 5444.
6 K. Uosaki, Y. Sato and H. Kita, *Langmuir*, 1991, **7**, 1510.
7 K. Uosaki, Y. Sato and H. Kita, *Langmuir*, 1991, **7**, 1170.
8 K, Shimazu, I. Yagi, Y. Sato and K. Uosaki, *J. Electroanal. Chem.*, 1994, **372**, 117.
9 K. Uosaki, Y. Sato and H. Kita, *Electrochim. Acta*, 1991, **36**, 1799.
10 Y. Sato, H. Itoigawa and K. Uosaki, *Bull. Chem. Soc. Jpn.*, 1993, **66**, 1032.
11 K. Kondo, S. Horiuchi, I. Yagi, S. Ye and K. Uosaki, *J. Am. Chem. Soc.*, 1999, **121**, 7155.
12 K. Shimazu, M. Takechi, H. Fujii, M. Suzuki, H. Saiki, T. Yoshimura and K. Uosaki, *Thin Solid Films*, 1996, **273**, 250.
13 H. Imahori, H. Norieda, H. Yamada, Y. Nishimura, I. Yamazaki, Y. Sakata and S. Fukuzumi, *J. Am. Chem. Soc.*, 2001, **123**, 100.
14 G. M. Ferrence, J. I. Henderson, D. G. Kurth, D. A. Morgenstern, T. Bein and C. P. Kubiak, *Langmuir*, 1996, **12**, 3075.
15 T. T. Ehler, N. Malmberg, K. Carron, B. P. Sullivan and L. J. Noe, *J. Phys. Chem. B*, 1997, **101**, 3174.
16 I. C. N. Diógenes, F. C. Nart and I. S. Moreita, *Inorg. Chem.*, 1999, **38**, 1646.
17 J. P. Collman, M. S. Ennis, D. A. Offord, L. L. Chng and J. H. Griffin, *Inorg. Chem.*, 1996, **35**, 1751.
18 J. Luo and S. S. Isied, *Langmuir*, 1998, **14**, 3602.
19 R. J. Forster, E. Figgemeier, A. C. Lees, J. Hjelm and J. G. Vos, *Langmuir*, 2000, **16**, 7867.
20 J. D. Tirado and H. D. Abruña, *J. Phys. Chem.*, 1996, **100**, 4556.
21 T. Inomata, M. Abe, T. Kondo, K. Umakoshi, K. Uosaki and Y. Sasaki, *Chem. Lett.*, 1999, 1097.
22 T. Inomata, H. Noda, M. Abe, T. Kondo, K. Uosaki, Y. Sasaki and M. Osawa, submitted for publication.
23 H. Takagi, A. Ichimura, T. Yano, I. Kinoshita, K. Isobe, M. Abe, Y. Sasaki, Y. Mikata, T. Tanase, N. Takeshita, C. Inoue, Y. Kimura, S. Endo, K. Tamura and S Yano, *Electrochemistry*, 1999, **67**, 1192.
24 M. Abe, T. Kondo, K. Uosaki and Y. Sasaki, *J. Electroanal. Chem.*, 1999, **473**, 93.
25 M. Abe, S. Ye, T. Kondo, K. Uosaki and Y. Sasaki, *Electrochemistry*, 1999, **67**, 1162.
26 M. Abe, A. Sato, T. Inomata, T. Kondo, K. Uosaki and Y. Sasaki, *J. Chem. Soc., Dalton Trans.*, 2000, 2693.
27 R. D. Cannon and R. P. White, *Prog. Inorg. Chem.*, 1988, **36**, 195.
28 J. A. Baumann, D. J. Salmon, S. T. Wilson, T. J. Meyer and W. E. Hatfield, *Inorg. Chem.*, 1978, **17**, 3342.
29 M. Abe, Y. Sasaki, Y. Yamada, K. Tsukahara, S. Yano and T. Ito, *Inorg. Chem.*, 1995, **34**, 4490.
30 M. Abe, Y. Sasaki, Y. Yamada, K. Tsukahara, S. Yano, T. Yamaguchi, M. Tominaga, I. Taniguchi and T. Ito, *Inorg. Chem.*, 1996, **35**, 6724.
31 T. Ito, T. Hamaguchi, H. Nagino, T. Yamaguchi, J. Washington and C. P. Kubiak, *Science*, 1997, **277**, 660.
32 T. Ito, T. Hamaguchi, H. Nagino, T. Yamaguchi, H. Kido, I. S. Zavarine, T. Richmond, J. Washington and C. P. Kubiak, *J. Am. Chem. Soc.*, 1999, **121**, 4625.
33 T. Yamaguchi, N. Imai, T. Ito and C. P. K. Kubiak, *Bull. Chem. Soc. Jpn.*, 2000, **73**, 1205.
34 H. Kido, H. Nagino and T. Ito, *Chem. Lett.*, 1996, 745.
35 H. E. Toma and A. D. P. Alexiou, *J. Braz. Chem. Soc.*, 1995, **6**, 267.
36 H. E. Toma and K. Araki, *Coord. Chem. Rev.*, 2000, **196**, 307.
37 S. Dovidauskas, H. E. Toma, K. Araki, H. C. Sacco and Y. Iamamoto, *Inorg. Chim. Acta*, 2000, **305**, 206.
38 H. E. Toma and S. Nikolaou, *J. Chem. Res.* (*S*), 2000, 326.
39 M. Abe, Y. Sasaki, A. Nagasawa and T. Ito, *Bull. Chem. Soc. Jpn.*, 1992, **65**, 1411.
40 Y. Sasaki, A. Nagasawa, A. Tokiwa-Yamamoto, A. Nagasawa and T. Ito, *Inorg. Chim. Acta*, 1993, **212**, 175.
41 G. Powell and D. T. Richens, *Inorg. Chim. Acta*, 1993, **213**, 147.
42 S. Davis and R. S. Drago, *Inorg. Chem.*, 1988, **27**, 4759.
43 S. A. Fouda and G. L. Rempel, *Inorg. Chem.*, 1979, **18**, 1.
44 D. A. Offord, S. B. Sachs, M. S. Ennis, T. A. Eberspacher, J. H. Griffin, C. E. D. Chidsey and J. P. Collman, *J. Am. Chem. Soc.*, 1998, **120**, 4478.
45 V. Huc, J. P. Bourgoin, C. Bureau, F. Valin, G. Zalczer and S. Palacin, *J. Phys. Chem. B*, 1999, **103**, 10489.
46 V. Huc, F. Armand, J. P. Bourgoin and S. Palacin, *Langmuir*, 2001, **17**, 1928.
47 K. Uosaki, S. Ye and T. Kondo, *J. Phys. Chem.*, 1995, **99**, 14117.
48 T. Kondo, S. Horiuchi, I. Yagi, S. Ye and K. Uosaki, *J. Am. Chem. Soc.*, 1999, **121**, 391.
49 J. A. Baumann, S. T. Wilson, D. J. Salmon, P. L. Hood and T. J. Meyer, *J. Am. Chem. Soc.*, 1979, **101**, 2916.
50 S. Ye, H. Akutagawa, K. Uosaki and Y. Sasaki, *Inorg. Chem.*, 1995, **34**, 4527.
51 A. J. Bard and L. R. Faulkner, *Electrochemical Methods, Fundamentals and Applications*, Wiley, New York, 1980.
52 M. Abe, M. Tanaka and Y. Sasaki, manuscript in preparation.
53 H. Kido, D. Akashi, Y. Sasaki and T. Ito, unpublished results.